

Clinical Significance of the Presence or Absence of Lipid-Rich Plaque Underneath Intact Fibrous Cap Plaque in Acute Coronary Syndrome

Masahiro Hoshino, MD; Taishi Yonetsu, MD; Eisuke Usui, MD; Yoshihisa Kanaji, MD; Hiroaki Ohya, MD; Yohei Sumino, MD; Masao Yamaguchi, MD; Masahiro Hada, MD; Rikuta Hamaya, MD; Yoshinori Kanno, MD; Tadashi Murai, MD, PhD; Tetsumin Lee, MD; Tsunekazu Kakuta, MD, PhD

Background—Although most coronary thromboses occur on the surface of lipid-rich plaque (LRP) with plaque rupture (PR), previous pathological and optical coherence tomography studies demonstrated diversity in the morphological characteristics of culprit plaque underlying the thrombus, including lesions with intact fibrous cap (IFC). We investigated the clinical significance of IFC in relation to the presence or absence of LRP observed via optical coherence tomography in culprit lesions of acute coronary syndrome.

Methods and Results—We investigated 510 patients with acute coronary syndrome who underwent optical coherence tomography for the culprit lesion. Optical coherence tomography analysis included the presence or absence of PR, which were categorized into the PR group and the IFC group, respectively. The IFC group was further categorized on the basis of the presence of LRP. Incidence of major adverse cardiac events (MACEs), including cardiac death, myocardial infarction, and clinically driven remote revascularizations, was compared. Culprit lesions were categorized into 328 PRs and 182 IFCs. MACEs occurred in 85 patients (16.7%) during the median follow-up duration of 621 days. LRP was detected in 325 lesions (99%) with PR, whereas 60 (33.0%) of the lesions with IFC did not show LRP. Kaplan-Meier analysis revealed significantly lower MACEs in the IFC group compared with the PR group. Furthermore, the IFC group without LRP showed significantly lower MACEs compared with the IFC group with LRP. Multivariate Cox proportional hazards analysis demonstrated that IFC without LRP was an independent predictor of better prognosis.

Conclusions—Exclusion of LRP underneath IFC culprit lesions in acute coronary syndrome may predict a lower risk of future MACEs. (*J Am Heart Assoc.* 2019;8:e011820. DOI: 10.1161/JAHA.118.011820.)

Key Words: acute coronary syndrome • intact fibrous cap • optical coherence tomography • percutaneous coronary intervention • plaque rupture

In the past decade, the clinical outcomes of patients with acute coronary syndrome (ACS) have dramatically improved because of the development of pharmacological and interventional therapies. Nevertheless, ACS remains one of the main causes of death globally. Pathological studies

have proposed 3 major mechanisms of coronary thrombosis causing ACS, including plaque rupture (PR), plaque erosion, and calcified nodule, of which PR is the most common phenotype.^{1,2} Although culprit plaques without evident PR (those with erosion or calcified nodules) account for approximately one third of ACS,^{3,4} their prevalence has been underestimated in clinical practice because of the limited ability of imaging modalities to identify these phenotypes, particularly in vivo. With the use of high-resolution images from optical coherence tomography (OCT), previous studies proposed an OCT definition of plaque erosion that is characterized by thrombosis overlying a plaque with intact fibrous cap (IFC). It has been reported that ACS caused by plaques with PR and IFC showed different morphological characteristics at both the culprit plaque and nonculprit plaques⁵; these plaques also yielded different clinical courses.^{6,7} A large lipid component, represented by a necrotic core, is one of the most important factors of vulnerable plaque, which is considered a precursor of coronary

From the Division of Cardiovascular Medicine, Tsuchiura Kyodo General Hospital, Ibaraki, Japan (M.H., E.U., Y.K., H.O., Y.S., M.Y., M.H., R.H., Y.K., T.M., T.K.); and Department of Cardiovascular Medicine, Tokyo Medical and Dental University, Tokyo, Japan (T.Y., T.L.).

Accompanying Data S1 and Table S1 are available at <https://www.ahajournals.org/doi/suppl/10.1161/JAHA.118.011820>

Correspondence to: Tsunekazu Kakuta, MD, PhD, Department of Cardiovascular Medicine, Tsuchiura Kyodo General Hospital, 4-1-1 Otsuno, Tsuchiura, Ibaraki 300-0028, Japan. E-mail: kaz@joy.email.ne.jp

Received December 18, 2018; accepted April 10, 2019.

© 2019 The Authors. Published on behalf of the American Heart Association, Inc., by Wiley. This is an open access article under the terms of the Creative Commons Attribution-NonCommercial-NoDerivs License, which permits use and distribution in any medium, provided the original work is properly cited, the use is non-commercial and no modifications or adaptations are made.

Clinical Perspective

What Is New?

- This optical coherence tomography study reports that lipid-rich plaque (LRP) was detected in almost all lesions with plaque rupture, whereas 33.0% of the lesions with intact fibrous cap did not show LRP features.
- In patients with acute coronary syndrome, the presence of LRP provides prognostic implication for adverse cardiac events, irrespective of the presence or absence of plaque rupture in the culprit lesion.
- Particularly, exclusion of LRP underneath intact fibrous cap culprit lesions in acute coronary syndrome provided better prognostic information after percutaneous coronary intervention.

What Are the Clinical Implications?

- Classification of culprit plaque morphological characteristics by using optical coherence tomography for both the presence or absence of plaque rupture and the presence of LRP underneath intact fibrous cap may be useful to stratify the risk for subsequent adverse events, which might help manage adjunctive therapeutic strategy and improve secondary prevention after percutaneous coronary intervention.

thrombosis.^{1,8,9} The existence of a necrotic core is essential for the onset of PR, followed by coronary thrombosis per the pathological definition of PR. However, plaque erosion may occur on the surface of the plaques, irrespective of the presence of a necrotic core,^{6,10} and little is known about the prevalence of the lipid component beneath plaque erosion and its impact on clinical outcomes. OCT enables the identification of plaque underlying coronary thrombosis, including lipid-rich plaque (LRP), which corresponds to a necrotic core or lipid pooling in histological analysis.¹¹ The aim of this study was to investigate the prevalence and clinical significance of LRP in patients with IFC who underwent percutaneous coronary intervention (PCI) and OCT evaluation of the culprit plaque.

Methods

The data that support the findings of this study are available from the corresponding author on reasonable request.

Study Population

The institutional database of intravascular OCT examinations performed at Tsuchiura Kyodo General Hospital (Ibaraki, Japan), between November 2008 and May 2017 (n=3192),

was retrospectively queried to identify patients of interest who met the following inclusion criteria: patients who underwent primary/urgent PCI for ACS and those with a consent for OCT examination of the culprit lesion during PCI and future data use and follow-up for the analysis. The culprit lesion was identified on the basis of coronary angiogram, ECG, or echocardiogram. Exclusion criteria were as follows: lesions requiring balloon angioplasty before OCT imaging; in-stent thrombosis, restenosis lesions, and bypass graft lesions; poor OCT image quality; patients with delayed presentation of >12 hours after onset; and patients in whom the culprit lesion could not be identified. Thus, the OCT images of 579 culprit lesions in 579 patients with ACS were analyzed in the present study (Figure 1).

Institutional exclusion criteria for OCT imaging in patients with ACS were cardiogenic shock, congestive heart failure, significant left main coronary artery disease, and suboptimal results after thrombectomy with TIMI (Thrombolysis in Myocardial Infarction) 0 to 2 flow. ST-segment–elevation myocardial infarction was defined as follows: continuous chest pain that lasted >30 minutes, arrival at the hospital within 12 hours from the onset of symptoms, ST-segment elevation >0.1 mV in >2 contiguous leads or new left bundle-branch block on a 12-lead ECG, and elevated cardiac markers. Non–ST-segment–elevation myocardial infarction was defined as ischemic symptoms in the absence of ST-segment elevation on ECG with elevated cardiac markers. Unstable angina was defined as angina at rest or one episode lasting >20 minutes during the preceding 48 hours and normal levels of cardiac markers. The primary outcome measure was major adverse cardiac events (MACEs), which is defined as a composite of cardiac death, acute myocardial infarction, and ischemia-driven remote revascularization (>3 months from the index PCI). Scheduled revascularization for nonculprit lesions that were identified in index coronary angiograms was not considered as a MACE. Device-oriented composite end point was defined as a composite of cardiac death, target-vessel myocardial infarction, and ischemia-driven target lesion remote revascularization.

This study was approved by the local ethics committee and conformed to the Declaration of Helsinki statement on research involving human subjects. Informed consent for registration into the institutional OCT database and potential future analysis of data were provided by all participants after thorough explanation of the protocol and potential risks related to imaging before catheterization.

OCT Image Acquisition and Analysis

OCT images were acquired before PCI procedures for lesions showing TIMI 3 flow without suspected angiographic thrombi and evaluated (Data S1). PR was defined as a plaque showing

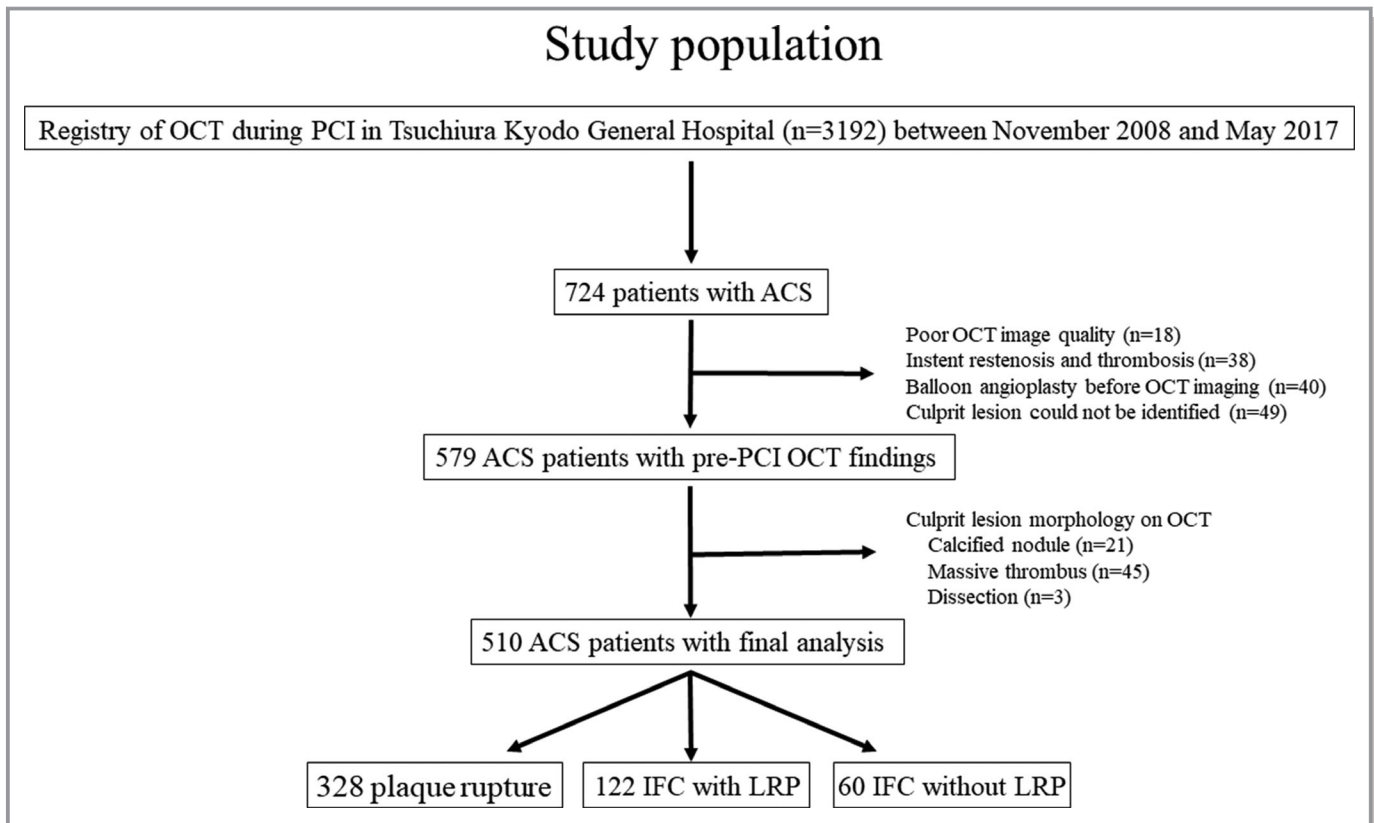


Figure 1. Study flow diagram illustrates the process of selecting patients for inclusion from the institutional database of intravascular optical coherence tomography (OCT) performed at Tsuchiura Kyodo General Hospital (Ibaraki, Japan) between November 2008 and May 2017. ACS indicates acute coronary syndrome; IFC, intact fibrous cap; LRP, lipid-rich plaque; PCI, percutaneous coronary intervention.

disruption of the fibrous cap with or without cavity formation. IFC was defined as a plaque where the fibrous cap of the culprit lesion was intact. Lipid was characterized as a diffusely bordered, signal-poor region underlying a signal-rich band that corresponded to the fibrous cap. For plaques with lipid, lipid length and arc were measured on the longitudinal reconstructed view or cross-sectional image by an independent investigator (E.U.). LRP was defined as a plaque with lipid having the maximal lipid arc ($>90^\circ$) and lipid length (>1 mm). In addition, thrombus length, maximal arc of the thrombus, and thrombus volume were measured according to the previous studies.¹² In brief, for the measurements of thrombus, OCT images were analyzed at 0.2-mm intervals. Thrombus area was traced by planimetry in frames with clear visualization of the vessel contours $>270^\circ$; otherwise, thrombus area was calculated by subtracting residual lumen area from the vessel contour area extrapolated from the nearest visible frames. Thrombus length was calculated by the number of frames with OCT thrombus multiplied by frame interval (0.2 mm). Thrombus arc was measured from the center of the residual lumen, and the maximum value was obtained as the maximum thrombus arc. Lesions with massive thrombus or calcified nodules were excluded from further analysis because

plaque morphological characteristics could not be identified in those with massive thrombus, and the pathological nature of calcified nodules is different from that of LRP. Thereafter, culprit lesions were divided into 3 categories, according to the OCT findings: lesions with PR (PR group), IFC with LRP (IFC-LRP group), and IFC without LRP (IFC-non-LRP group) (Figure 2).

Angiography Analysis

Baseline coronary angiograms obtained before OCT image acquisition or interventional procedures were analyzed with offline software (QAngio XA 7.3; Medis, Leiden, the Netherlands). Angiographic lesion morphological characteristics were classified according to the American Heart Association/American College of Cardiology lesion classification.¹³

Statistical Analysis

Categorical values are presented as counts and proportions, and comparisons between groups were performed using the χ^2 test or Fisher's exact test, depending on the data. Continuous values, showing a normal distribution, are

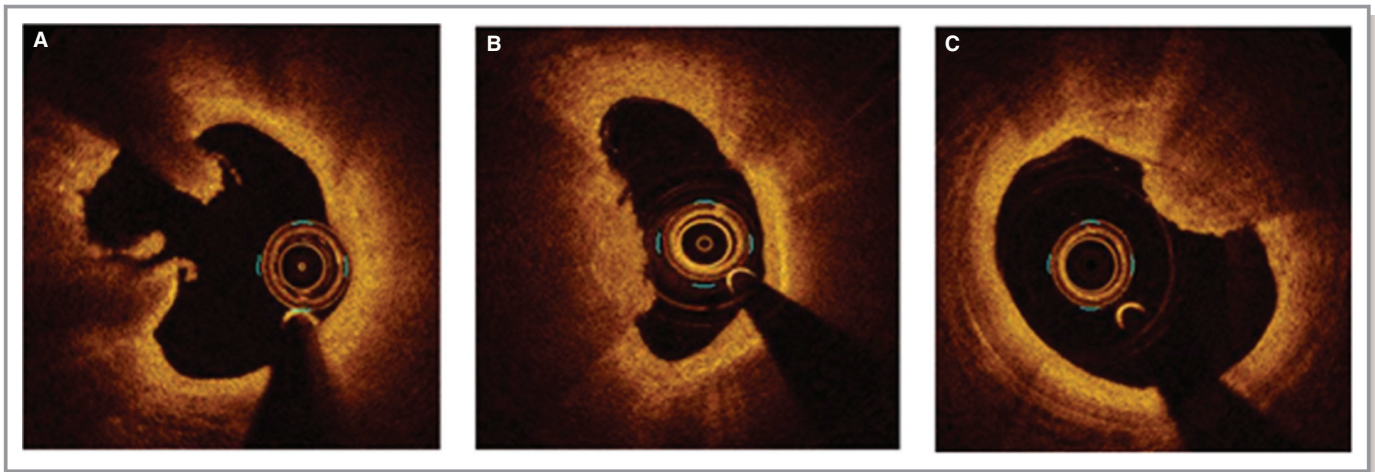


Figure 2. Representative optical coherence tomography (OCT) images of 3 types of culprit plaque morphological characteristics in patients with acute coronary syndrome (ACS). Representative OCT images of ACS. **A**, Lesions with plaque rupture; cross-sectional image shows rupture of fibrous cap and a cavity formation in the lipid core. **B**, Lesions with intact fibrous cap (IFC)–lipid-rich plaque (LRP); LRP and thrombus without disruption of fibrous cap. **C**, Lesions with IFC–non-LRP; fibrous plaque and thrombus without disruption of fibrous cap.

expressed as mean±SD; and Student *t* test was performed to compare the values among groups. Nonnormally distributed, continuous values are expressed as median (25th–75th percentile), and the Mann-Whitney *U* test was used to compare between the groups. The Kruskal-Wallis test was performed to compare continuous variables among the 3 groups; post hoc comparisons were performed using pairwise comparisons between groups. Intraobserver and interobserver variabilities for categorical OCT variables were estimated using the κ coefficient. Survival curves using the Kaplan-Meier methods were produced for the presence of PR, LRP, or massive thrombus as the culprit lesion; and they were compared using the log-rank test. The predictors of MACEs were determined using the Cox proportional hazards regression model. The covariates used in multivariate analysis were selected using the criterion of $P < 0.20$ in the univariate analysis. The proportional hazards assumption was checked using statistical tests and graphical diagnostics based on the scaled Schoenfeld residuals. A collinearity index was used for checking linear combinations among covariates, and the Akaike information criterion was used for avoiding overfitting. All statistical analyses were performed with SPSS 18.0 (SPSS Inc, Chicago, IL) and R, version 3.0.2 (The R Foundation for Statistical Computing, Vienna, Austria). $P < 0.05$ was considered statistically significant.

Results

Patient Characteristics and Angiographic and Procedural Findings

Of 579 culprit lesions of ACS analyzed in the present study, underlying plaque morphological characteristics could not be

categorized via OCT in 69 lesions because of massive thrombus ($n=45$), calcified nodule ($n=21$), or spontaneous coronary dissection ($n=3$). After excluding these lesions, 510 culprit lesions of ACS were included in the final analysis. In the subsequent OCT analysis, 328 lesions (64.3%) were categorized into the PR group, 122 lesions (23.9%) were categorized into the IFC-LRP group, and 60 lesions (11.8%) were categorized into the IFC–non-LRP group (Figure 1). Clinical characteristics of the PR, IFC-LRP, and IFC–non-LRP groups are summarized in Table 1. Angiographic and procedural data are summarized in Table 2.

OCT Findings

OCT findings were compared among the 3 groups (Table 3). Compared with IFC-LRP, lesions with PR had significantly thinner fibrous caps, more frequent thin-cap fibroatheroma, longer lipid length, and greater maximum lipid arc at the culprit lesion. Culprit lesions with PR had significantly greater volume of OCT-defined thrombus than those with IFC-LRP or IFC–non-LRP. The intraobserver and interobserver κ values for the qualitative assessments of PR were 0.89 and 0.87, respectively; for LRP assessment, they were 0.88 and 0.85, respectively.

Follow-Up Data

During a median follow-up duration of 621 days (range, 415–1589 days), 85 patients (16.7%) experienced MACEs. The numbers of adverse events are summarized in Table 4, and the comparison of patient characteristics between those with and without MACEs is summarized in Table S1. Second-generation, drug-eluting stents were used less frequently in

Table 1. Patient Characteristics

Characteristics	PR Group (n=328)	IFC-LRP Group (n=122)	IFC-Non-LRP Group (n=60)	P Value
Age, y	67.0 (58.0–74.0)	68.0 (58.3–73.0)	67.0 (55.0–74.0)	0.728
Men	264 (80.5)	97 (79.5)	42 (70.0)	0.184
Hypertension	213 (64.9)	83 (68.0)	40 (66.7)	0.820
Dyslipidemia	160 (48.8)	63 (51.6)	30 (50.0)	0.863
Diabetes mellitus	105 (32.0)	43 (35.2)	20 (33.3)	0.808
Current smoker	133 (40.5)	55 (45.1)	31 (51.7)	0.240
Clinical presentation				
STEMI	171 (52.1)	29 (23.8)	19 (31.7)	<0.001 ^{*,†,‡}
NSTEMI	131 (39.9)	63 (51.6)	36 (60.0)	
Unstable angina	26 (7.9)	30 (24.5)	5 (8.3)	
Prior PCI	32 (9.8)	9 (7.4)	4 (6.7)	0.709
Prior MI	24 (7.3)	5 (4.1)	4 (6.7)	0.503
LDL cholesterol, mg/dL	122.0 (99.0–144.0)	124.0 (99.0–144.0)	111.0 (94.8–134.8)	0.326
HDL cholesterol, mg/dL	44.0 (38.0–51.0)	45.0 (39.0–53.0)	48.0 (40.5–57.0)	0.073
eGFR, mL/min per 1.73 m ²	72.6 (58.0–84.2)	73.8 (64.5–87.0)	69.1 (52.0–85.7)	0.068
CRP, mg/dL	0.15 (0.05–0.50)	0.16 (0.04–0.52)	0.12 (0.06–0.44)	0.973
Medication				
Prior aspirin use	60 (18.3)	25 (20.5)	12 (20.0)	0.851
Prior statin use	70 (21.3)	25 (20.5)	16 (26.7)	0.607

Data are presented as number (percentage) or median (quartile 1–quartile 3). CRP indicates C-reactive protein; eGFR, estimated glomerular filtration rate; HDL, high-density lipoprotein; IFC, intact fibrous cap; LDL, low-density lipoprotein; LRP, lipid-rich plaque; MI, myocardial infarction; NSTEMI, non-ST-segment-elevation MI; PCI, percutaneous coronary intervention; PR, plaque rupture; STEMI, ST-segment-elevation MI.

* $P < 0.05$ for PR vs IFC-LRP, [†] $P < 0.05$ for PR vs IFC-non-LRP, [‡] $P < 0.05$ for IFC-LRP vs IFC-non-LRP by post hoc test.

patients with MACEs than in those without. American Heart Association/American College of Cardiology type B2/C lesions, LRP via OCT, and thin-cap fibroatheroma via OCT were more frequently observed in patients with MACEs than in those without MACEs. Kaplan-Meier analysis revealed that MACE-free survival rate was significantly higher in the IFC group, which combined the IFC-LRP and IFC-non-LRP groups, than in the PR group ($P=0.005$) (Figure 3A). When we stratified patients according to the existence of LRP in the OCT image of the culprit lesion, MACE-free survival rate was significantly worse in patients with LRP than in those without LRP ($P=0.005$) (Figure 3B). Moreover, in patients with a culprit lesion with IFC, a significantly higher MACE-free survival rate was observed in the IFC-non-LRP group compared with the IFC-LRP group ($P=0.037$) (Figure 4A), and a significantly lower device-oriented composite end point rate was observed in the IFC-non-LRP group compared with the IFC-LRP group ($P=0.047$) (Figure 4B). The incidence of MACEs was significantly higher in association with the increase in the quadrant of maximal lipid arc in patients with IFC (Figure 5).

The multivariate Cox proportional hazard analysis demonstrated that culprit lesion morphological characteristics of

IFC-non-LRP on OCT, use of second-generation drug-eluting stents, estimated glomerular filtration rate, and culprit lesion with American Heart Association/American College of Cardiology type B2/C were independent predictors of MACEs (Table 5). In this model, no violation of proportional hazard over time was detected. MACE-free survival rate was significantly preferable in patients with IFC-LRP than in those with IFC-non-LRP (Figure 6A). Moreover, patients with massive thrombus were associated with poor prognosis, similarly to the patients with PR (Figure 6B).

Discussion

To the best of our knowledge, this is the first study demonstrating the prognostic significance of LRP in culprit lesions with IFC defined via OCT. Major findings of the present study were as follows: (1) the vast majority of culprit lesions with PR exhibited LRP using OCT, whereas approximately one third of the lesions with IFC did not show LRP; (2) MACE-free survival rate was significantly worse in patients with PR than in those with IFC; (3) MACE-free survival rate was significantly worse in patients with LRP in culprit lesions compared with

Table 2. Angiographic and Procedural Data

Variable	PR Group (n=328)	IFC-LRP Group (n=122)	IFC-Non-LRP Group (n=60)	P Value
Lesion location				
RCA	132	33	12	0.005 [†]
LAD	135	63	37	
LCX	61	26	11	
Quantitative coronary angiography data				
Reference diameter, mm	2.78 (2.40–3.22)	2.70 (2.34–3.00)	2.91 (2.38–3.24)	0.263
Minimum lumen diameter, mm	0.53 (0.00–0.79)	0.64 (0.46–0.80)	0.65 (0.14–0.98)	0.009*
Diameter stenosis, %	80.5 (71.2–100.0)	76.8 (68.9–83.1)	76.0 (61.9–93.0)	0.003*
Lesion length, mm	13.3 (10.0–16.6)	12.1 (9.9–16.9)	9.9 (8.3–12.8)	<0.001 ^{†,‡}
ACC/AHA classification B2/C	170 (51.8)	41 (33.6)	22 (36.7)	<0.001 ^{†,‡}
TIMI flow grade				
Pre-PCI TIMI 0–2	196 (64.9)	51 (43.2)	32 (55.2)	<0.001*
Post-PCI TIMI 0–2	40 (13.2)	4 (4.3)	6 (10.9)	0.048
Multivessel disease	121 (36.9)	45 (36.9)	13 (21.7)	0.068
Stent				
Stent size, mm	3.5 (3.0–3.5)	3.38 (3.0–3.5)	3.5 (3.0–3.5)	0.023*
Stent length, mm	24.0 (19.0–33.0)	24.0 (19.0–33.0)	20.0 (16.0–28.0)	0.011 ^{†,‡}
DES	200	87	36	<0.001 ^{†,‡}
BMS	123	31	10	
POBA/aspiration	4	3	13	
Second-generation DES	175 (53.4)	68 (55.7)	35 (58.3)	0.739

Data are presented as number (percentage) or median (quartile 1–quartile 3). ACC indicates American College of Cardiology; AHA, American Heart Association; BMS, bare-metal stent; DES, drug-eluting stent; IFC, intact fibrous cap; LAD, left anterodescending artery; LCX, left circumflex; LRP, lipid-rich plaque; PCI, percutaneous coronary intervention; POBA, plain old balloon angioplasty; PR, plaque rupture; RCA, right coronary artery; TIMI, Thrombolysis in Myocardial Infarction.

* $P < 0.05$ for plaque rupture vs IFC with LRP, [†] $P < 0.05$ for plaque rupture vs IFC without LRP, [‡] $P < 0.05$ for IFC with LRP vs IFC without LRP.

those without LRP; and (4) MACE-free survival was significantly preferable in patients with IFC showing no LRP than in those with IFC with LRP.

Differing Clinical Courses Based on Different Morphological Plaque Characteristics

Previous OCT studies demonstrated that the patients with ACS exhibiting IFC in the culprit lesions showed preferable clinical outcomes after PCI compared with those with PR.^{6,7} Niccoli et al investigated 139 patients with ACS, in whom the culprit lesions were categorized into PR (n=82) and IFC (n=57).⁶ The researchers reported that MACE was significantly more frequent in patients with PR, which is consistent with the present study. In our previous OCT study comprising 318 patients with ACS (141 patients with PR and 131 patients with IFC), we showed a lower rate of clinical cardiac events in patients with IFC than in those with PR.⁷ In both previous studies,^{6,7} each adverse event besides target vessel revascularization showed a nonsignificant trend toward a

higher incidence in patients with PR, which potentially indicates greater atheromatous burden not only in the culprit vessels, but also in nonculprit vessels of patients with PR compared with those with IFC. In fact, previous OCT and computed tomography studies showed that patients with ACS with concurrent PR in the culprit lesion exhibited vulnerable plaque morphological characteristics in nonculprit lesions or nonculprit vessels.^{14–16} In the present study, macrophage infiltration was significantly less in the IFC group without lipid than in the other 2 groups. Macrophage degradation of fibrous cap is an important contributor to atherosclerotic plaque instability. Previous reports showed a significantly higher macrophage density at the rupture site and LRP site.¹⁷ Moreover, macrophage was associated with arterial wall lipid deposition contributing to inflammatory processes.¹⁸ Previous reports also showed more macrophage volume suggested the extent of initial coronary plaque inflammation and had a possible role for the recurrence of angina after PCI.^{19,20} Therefore, our finding that macrophage infiltration was significantly less in the IFC–non-LRP group

Table 3. Pre-PCI OCT Findings

Findings	PR Group (n=328)	IFC-LRP Group (n=122)	IFC-Non-LRP Group (n=60)	P Value
Thrombus	274 (83.5)	74 (60.7)	29 (48.3)	<0.001* [†]
TCFA	211 (64.5)	43 (35.2)	...	<0.001
LRP	325 (99.1)	122 (100)
Calcified plaque	124 (37.8)	47 (38.5)	25 (41.7)	0.848
Macrophage	236 (72.0)	79 (64.8)	22 (36.7)	<0.001 ^{†,‡}
Fibrous cap thickness, μm	63 (57–80)	83 (60–120)	...	<0.001
Max lipid arc, $^{\circ}$	246.8 (205.4–294.6)	229.5 (192.7–273.9)	...	0.020
Lipid length, mm	8.1 (5.3–11.9)	5.6 (3.7–8.1)	...	<0.001
Thrombus volume, mm^3	0.76 (0.06–2.45)	0.11 (0.0–0.45)	0.0 (0.0–0.59)	<0.001* [†]
Thrombus length, mm	2.9 (0.8–5.3)	1.1 (0.0–2.6)	0.0 (0.0–2.1)	<0.001* [†]
Maximum thrombus arc, $^{\circ}$	108.1 (45.3–158.5)	53.8 (0.0–120.3)	0.0 (0.0–99.3)	<0.001* [†]

Data are presented as number (percentage) or median (quartile 1–quartile 3). IFC indicates intact fibrous cap; LRP, lipid-rich plaque; OCT, optical coherence tomography; PCI, percutaneous coronary intervention; PR, plaque rupture; TCFA, thin-cap fibroatheroma.

* $P<0.05$ for plaque rupture vs IFC with LRP, [†] $P<0.05$ for plaque rupture vs IFC without LRP, [‡] $P<0.05$ for IFC with LRP vs IFC without LRP.

than in the other 2 groups in patients with ACS might be linked with better prognosis after PCI.

Clinical Implications of LRP

Vulnerable plaque, which is generally defined as a plaque prone to rupture, is associated with a large necrotic core and thin fibrous cap, modified by inflammatory activities within the plaque.^{1,21} Therefore, plaque with a large lipid component is considered a precursor of cardiac events, which was elucidated in recent studies using intracoronary imaging modalities.^{8,9,22,23} The PROSPECT (Providing Regional Observations to Study Predictors of Events in the Coronary Tree) study,²² in which patients presenting with ACS underwent 3-vessel virtual histological intravascular ultrasound after successful PCI,

demonstrated that thin-cap fibroatheroma in nonculprit lesions, indicated via virtual histological intravascular ultrasound, was associated with future cardiac events. On the other hand, a subgroup analysis from the PROSPECT study showed that lesions without fibroatheroma were clinically stable and were rarely associated with clinical events during 3 years of follow-up.²⁴ Conversely, Xing et al showed that in patients with LRP, identified via OCT at the nonculprit region of the coronary artery, LRP was associated with a higher MACE rate in comparison to those without LRP.⁸ In the present study, patients exhibiting LRP using OCT in the culprit lesion showed worse clinical outcomes compared with those without LRP (Figure 3B), which might be plausible considering the impact of LRP on future coronary events and the association between culprit lesion morphological characteristics and nonculprit lesion morphological

Table 4. Clinical Events During the Follow-Up Period

Clinical Event	PR Group (n=328)	IFC-LRP Group (n=122)	IFC-Non-LRP Group (n=60)	P Value
MACE	65 (19.8)	18 (14.8)	2 (3.3)	0.002
Cardiac death	10	1	0	0.288
Nonfatal myocardial infarction	4	0	0	0.745
TVR	31	11	1	0.106
Non-TVR	20	6	1	0.420
DOCE	45 (13.7)	12 (9.8)	1 (0.02)	0.011
Cardiac death	8	1	0	0.452
Nonfatal myocardial infarction	5	0	0	0.491
TVR	32	11	1	0.101

Data are presented as number (percentage). DOCE indicates device-oriented composite end point; IFC, intact fibrous cap; LRP, lipid-rich plaque; MACE, major advance cardiac event; PR, plaque rupture; TVR, target vessel revascularization.

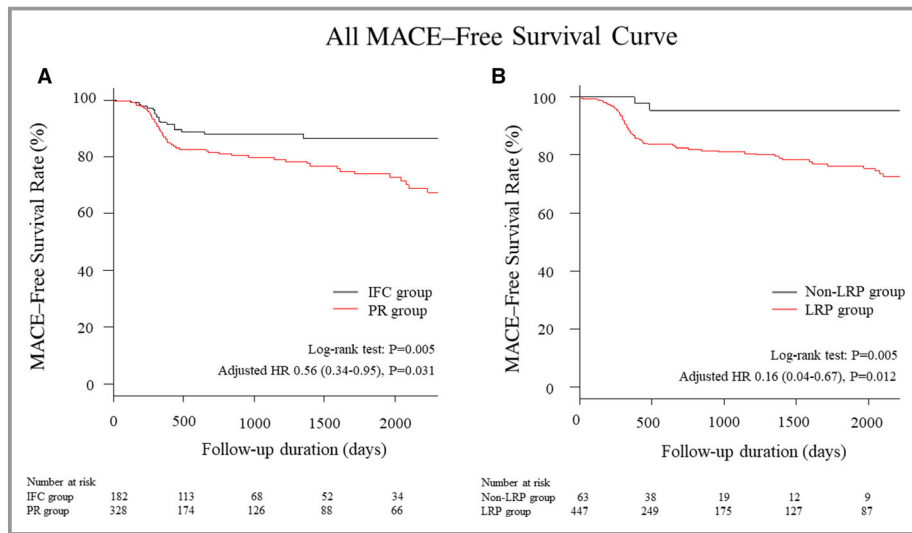


Figure 3. Kaplan-Meier curves showing major adverse cardiac event (MACE)-free survival, according to the culprit plaque morphological characteristics. **A**, The incidence of MACEs was significantly higher in patients with plaque rupture (PR) than in those with intact fibrous cap (IFC). Compared with patients with PR, the adjusted hazard ratio (HR) of those with IFC was generated from multivariate Cox proportional hazards model, including estimated glomerular filtration rate (eGFR), prior myocardial infarction (MI), second-generation drug-eluting stent (DES), and American Heart Association/American College of Cardiology (AHA/ACC) classification B2/C. **B**, The incidence of MACEs was significantly higher in patients with lipid-rich plaque (LRP) than in those without LRP. Compared with patients with LRP, the adjusted HR of those without LRP was generated from multivariate Cox proportional hazards model, including eGFR, prior MI, second-generation DES, and AHA/ACC classification B2/C.

characteristics.^{8,14,15} Moreover, in the present study, even if we selected the patients with plaques with IFC in the culprit lesions, the presence of LRP in the culprit lesion was associated with

worse clinical outcomes in terms of composite adverse events (Figure 4A), which is primarily driven by revascularization for recurrent ischemia (Figure 4B).

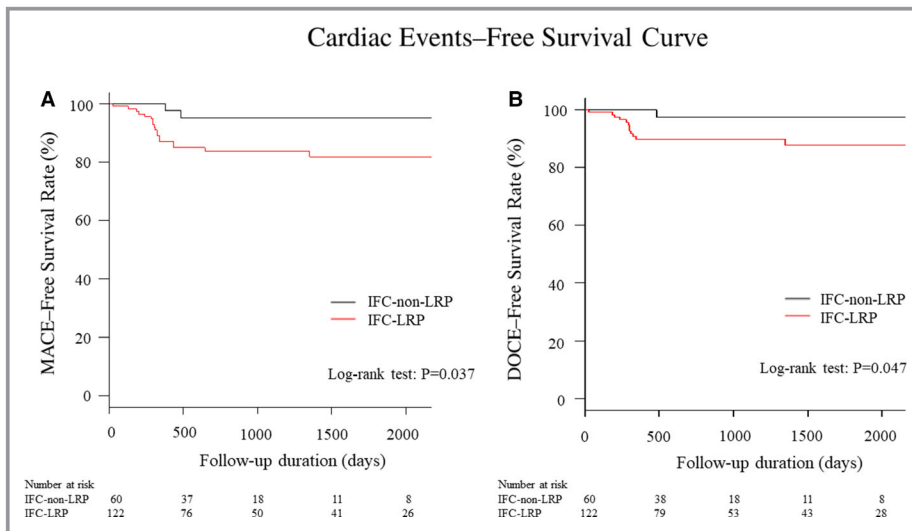


Figure 4. Kaplan-Meier curves showing major adverse cardiac event (MACE)-free survival according to the presence or absence of lipid-rich plaque (LRP) in patients with intact fibrous cap (IFC). Compared with patients with IFC-non-LRP, patients with IFC-LRP had the higher incidence of MACEs (**A**) and device-oriented composite end point (DOCE; **B**). Compared with patients with IFC-LRP, adjusted hazard ratio (HR) of those with IFC-non-LRP was generated from multivariate Cox proportional hazards models, including hyperlipidemia and second-generation drug-eluting stents.

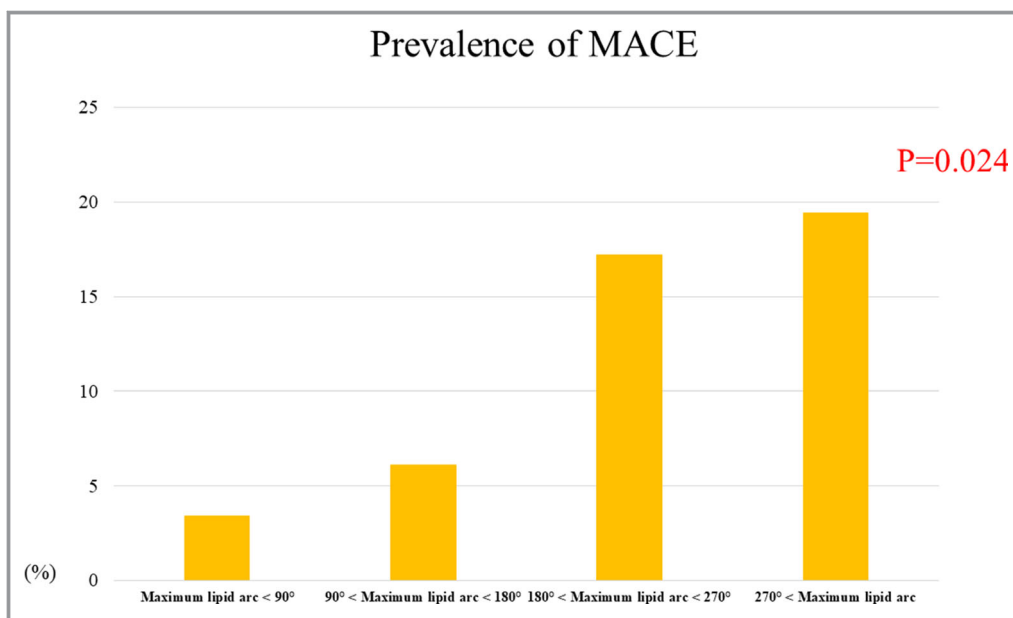


Figure 5. Incidence of major adverse cardiac events (MACEs) among 4 quadrants of maximum lipid arc, defined by optical coherence tomography (OCT) in patients with intact fibrous cap (IFC). Frequency of MACEs, according to each quadrant of maximum lipid arc defined by OCT in patients with IFC. When patients with IFC were divided into quadrants by maximum lipid arc defined by OCT, the frequency of MACEs was significantly higher in the larger maximum lipid arc.

Study Limitations

First, this study was a retrospective, observational study at a single center; therefore, selection bias may have influenced the results and the results may not be generalizable. Second,

because of the wide range of the study period, adherence to optimal medical therapy was not excellent in the early period of the study. Third, the final decision to perform OCT examination was at the operator’s discretion. Furthermore, as shown in the

Table 5. Univariate and Multivariate Cox Proportional Hazards Analysis for MACEs

Variable	Univariate Analysis			Multivariate Analysis		
	HR	95% CI	P Value	HR	95% CI	P Value
OCT-LRP	5.86	1.44–23.83	0.014
OCT-TCFA	1.92	1.21–3.03	0.005
OCT-PR	2.06	1.23–3.43	0.006
eGFR	0.99	0.98–1.00	0.046	0.99	0.98–1.00	0.032
Prior MI	1.74	0.87–3.49	0.116	1.74	0.86–3.53	0.123
Multivessel disease	1.37	0.89–2.11	0.155
Second-generation DES	0.58	0.37–0.92	0.021	0.61	0.38–0.97	0.038
Stent length	1.01	1.00–1.03	0.146
AHA/ACC classification B2/C	1.85	1.19–2.87	0.006	1.70	1.09–2.67	0.021
Statin at discharge	0.64	0.37–1.10	0.108
Culprit lesion morphological characteristics on OCT						
PR	Reference	Reference
IFC-LRP	0.67	0.39–1.12	0.127	0.81	0.47–1.37	0.426
IFC-non-LRP	0.16	0.04–0.67	0.012	0.17	0.04–0.70	0.014

ACC indicates American College of Cardiology; AHA, American Heart Association; DES, drug-eluting stent; eGFR, estimated glomerular filtration rate; HR, hazard ratio; IFC, intact fibrous cap; LRP, lipid-rich plaque; MACE, major adverse cardiac event; MI, myocardial infarction; OCT, optical coherence tomography; PR, plaque rupture; TCFA, thin-cap fibroatheroma.

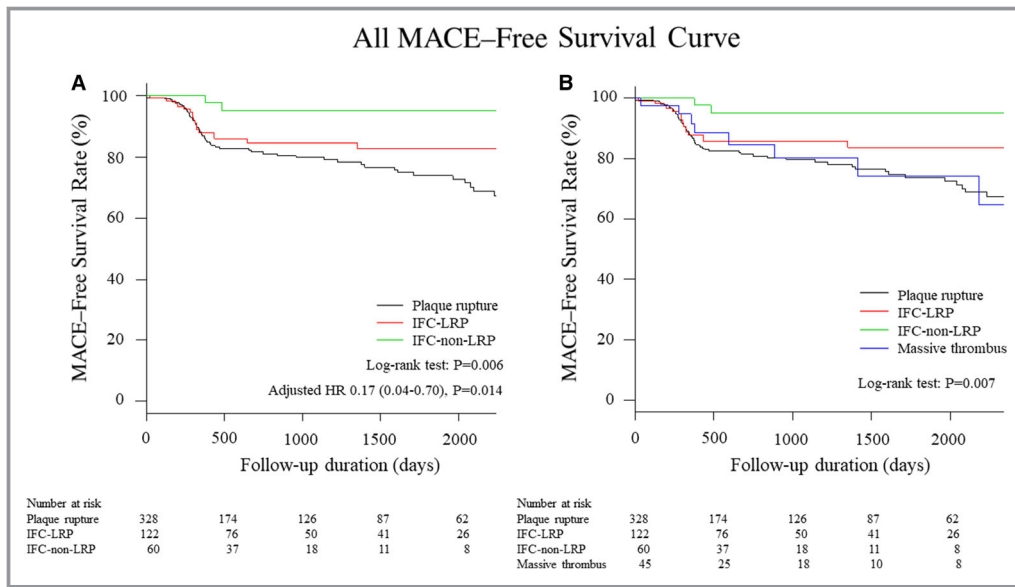


Figure 6. Kaplan-Meier curves showing major adverse cardiac event (MACE)-free survival classified by culprit plaque morphological characteristics by optical coherence tomography. Either 3-group (A) or 4-group (B) classifications of culprit plaque morphological characteristics can discriminate high-risk patients for future MACEs after percutaneous coronary intervention. Compared with patients with plaque rupture, adjusted hazard ratio (HR) of those with intact fibrous cap (IFC)-non-lipid-rich plaque (LRP) was generated from multivariate Cox proportional hazards model, including estimated glomerular filtration rate, prior myocardial infarction, second-generation drug-eluting stents, and American Heart Association/American College of Cardiology classification B2/C.

Methods section, OCT was not performed in patients with cardiogenic shock, congestive heart failure, significant left main disease, and TIMI 0 to 2 flow after thrombectomy because of safety concerns, which may have led to selection bias. Fourth, ACS with calcified nodules was excluded from the analysis to avoid confusion about the definition of IFC. Fifth, the presence of thrombus overlying the culprit lesion might have reduced the accuracy to assess the underlying plaque characteristics by OCT. Finally, because the identification of small PR in the thrombotic event is often difficult, PR might have been misdiagnosed as IFC in certain cases. This is an important limitation of OCT-derived plaque categorization.

Conclusions

In patients with culprit lesions with IFC, the presence of LRP via OCT was significantly associated with an increased risk for future MACEs compared with those with IFC without LRP, which is primarily driven by revascularization for recurrent ischemia. Classification of culprit plaque morphological characteristics via OCT for both the presence or absence of PR and the underlying presence of LRP underneath IFC may be useful to stratify the risk for subsequent adverse events.

Disclosures

None.

References

- Virmani R, Burke AP, Farb A, Kolodgie FD. Pathology of the vulnerable plaque. *J Am Coll Cardiol.* 2006;47:C13-C18.
- Burke AP, Farb A, Malcom GT, Liang YH, Smialek J, Virmani R. Coronary risk factors and plaque morphology in men with coronary disease who died suddenly. *N Engl J Med.* 1997;336:1276-1282.
- White SJ, Newby AC, Johnson TW. Endothelial erosion of plaques as a substrate for coronary thrombosis. *Thromb Haemost.* 2016;115:509-519.
- Durand E, Scoazec A, Lafont A, Bodaert J, Al Hajzen A, Addad F, Mirshahi M, Desnos M, Tedgui A, Mallat Z. In vivo induction of endothelial apoptosis leads to vessel thrombosis and endothelial denudation: a clue to the understanding of the mechanisms of thrombotic plaque erosion. *Circulation.* 2004;109:2503-2506.
- Fujii K, Kobayashi Y, Mintz GS, Takebayashi H, Dangas G, Moussa I, Mehran R, Lansky AJ, Kreps E, Collins M, Colombo A, Stone GW, Leon MB, Moses JW. Intravascular ultrasound assessment of ulcerated ruptured plaques: a comparison of culprit and nonculprit lesions of patients with acute coronary syndromes and lesions in patients without acute coronary syndromes. *Circulation.* 2003;108:2473-2478.
- Niccoli G, Montone RA, Di Vito L, Gramagna M, Refaat H, Scalone G, Leone AM, Trani C, Burzotta F, Porto I, Aurigemma C, Prati F, Crea F. Plaque rupture and intact fibrous cap assessed by optical coherence tomography portend different outcomes in patients with acute coronary syndrome. *Eur Heart J.* 2015;36:1377-1384.
- Yonetsu T, Lee T, Murai T, Suzuki M, Matsumura A, Hashimoto Y, Kakuta T. Plaque morphologies and the clinical prognosis of acute coronary syndrome caused by lesions with intact fibrous cap diagnosed by optical coherence tomography. *Int J Cardiol.* 2016;203:766-774.
- Xing L, Higuma T, Wang Z, Aguirre AD, Mizuno K, Takano M, Dauerman HL, Park SJ, Jang Y, Kim CJ, Kim SJ, Choi SY, Itoh T, Uemura S, Lowe H, Walters DL, Barlis P, Lee S, Lerman A, Toma C, Tan JWC, Yamamoto E, Bryniarski K, Dai J, Zanchin T, Zhang S, Yu B, Lee H, Fujimoto J, Fuster V, Jang IK. Clinical significance of lipid-rich plaque detected by optical coherence tomography: a 4-year follow-up study. *J Am Coll Cardiol.* 2017;69:2502-2513.
- Oemrawsingh RM, Cheng JM, Garcia-Garcia HM, van Geuns RJ, de Boer SP, Simsek C, Kardys I, Lenzen MJ, van Domburg RT, Regar E, Serruys PW, Akkerhuis KM, Boersma E; ATHEROREMO-NIRS Investigators. Near-infrared spectroscopy predicts cardiovascular outcome in patients with coronary artery disease. *J Am Coll Cardiol.* 2014;64:2510-2518.

10. Jia H, Abtahian F, Aguirre AD, Lee S, Chia S, Lowe H, Kato K, Yonetsu T, Vergallo R, Hu S, Tian J, Lee H, Park SJ, Jang YS, Raffel OC, Mizuno K, Uemura S, Itoh T, Kakuta T, Choi SY, Dauerman HL, Prasad A, Toma C, McNulty I, Zhang S, Yu B, Fuster V, Narula J, Virmani R, Jang IK. In vivo diagnosis of plaque erosion and calcified nodule in patients with acute coronary syndrome by intravascular optical coherence tomography. *J Am Coll Cardiol*. 2013;62:1748–1758.
11. Yabushita H, Bouma BE, Houser SL, Aretz HT, Jang IK, Schlerendorf KH, Kauffman CR, Shishkov M, Kang DH, Halpern EF, Tearney GJ. Characterization of human atherosclerosis by optical coherence tomography. *Circulation*. 2002;106:1640–1645.
12. Higuma T, Soeda T, Yamada M, Yokota T, Yokoyama H, Izumiyama K, Nishizaki F, Minami Y, Xing L, Yamamoto E, Lee H, Okumura K, Jang IK. Does residual thrombus after aspiration thrombectomy affect the outcome of primary PCI in patients with ST-segment elevation myocardial infarction? An optical coherence tomography study. *JACC Cardiovasc Interv*. 2016;9:2002–2011.
13. Kastrati A, Schomig A, Elezi S, Dirschinger J, Mehilli J, Schuhlen H, Blasini R, Neumann FJ. Prognostic value of the modified American College of Cardiology/American Heart Association stenosis morphology classification for long-term angiographic and clinical outcome after coronary stent placement. *Circulation*. 1999;100:1285–1290.
14. Vergallo R, Ren X, Yonetsu T, Kato K, Uemura S, Yu B, Jia H, Abtahian F, Aguirre AD, Tian J, Hu S, Soeda T, Lee H, McNulty I, Park SJ, Jang Y, Prasad A, Lee S, Zhang S, Porto I, Biasucci LM, Crea F, Jang IK. Pancoronary plaque vulnerability in patients with acute coronary syndrome and ruptured culprit plaque: a 3-vessel optical coherence tomography study. *Am Heart J*. 2014;167:59–67.
15. Sugiyama T, Yamamoto E, Bryniarski K, Xing L, Lee H, Isobe M, Libby P, Jang IK. Nonculprit plaque characteristics in patients with acute coronary syndrome caused by plaque erosion vs plaque rupture: a 3-vessel optical coherence tomography study. *JAMA Cardiol*. 2018;3:207–214.
16. Ozaki Y, Okumura M, Ismail TF, Motoyama S, Naruse H, Hattori K, Kawai H, Sarai M, Takagi Y, Ishii J, Anno H, Virmani R, Serruys PW, Narula J. Coronary CT angiographic characteristics of culprit lesions in acute coronary syndromes not related to plaque rupture as defined by optical coherence tomography and angiography. *Eur Heart J*. 2011;32:2814–2823.
17. MacNeill BD, Jang IK, Bouma BE, Iftimia N, Takano M, Yabushita H, Shishkov M, Kauffman CR, Houser SL, Aretz HT, DeJoseph D, Halpern EF, Tearney GJ. Focal and multi-focal plaque macrophage distributions in patients with acute and stable presentations of coronary artery disease. *J Am Coll Cardiol*. 2004;44:972–979.
18. Xu XH, Shah PK, Faure E, Equils O, Thomas L, Fishbein MC, Luthringer D, Xu XP, Rajavashisth TB, Yano J, Kaul S, Arditi M. Toll-like receptor-4 is expressed by macrophages in murine and human lipid-rich atherosclerotic plaques and upregulated by oxidized LDL. *Circulation*. 2001;104:3103–3108.
19. Moreno PR, Bernardi VH, Lopez-Cuellar J, Newell JB, McMellon C, Gold HK, Palacios IF, Fuster V, Fallon JT. Macrophage infiltration predicts restenosis after coronary intervention in patients with unstable angina. *Circulation*. 1996;94:3098–3102.
20. Meuwissen M, Piek JJ, van der Wal AC, Chamuleau SA, Koch KT, Teeling P, van der Loos CM, Tijssen JG, Becker AE. Recurrent unstable angina after directional coronary atherectomy is related to the extent of initial coronary plaque inflammation. *J Am Coll Cardiol*. 2001;37:1271–1276.
21. Sato Y, Hatakeyama K, Yamashita A, Marutsuka K, Sumiyoshi A, Asada Y. Proportion of fibrin and platelets differs in thrombi on ruptured and eroded coronary atherosclerotic plaques in humans. *Heart*. 2005;91:526–530.
22. Stone GW, Maehara A, Lansky AJ, de Bruyne B, Cristea E, Mintz GS, Mehran R, McPherson J, Farhat N, Marso SP, Parise H, Templin B, White R, Zhang Z, Serruys PW; PROSPECT Investigators. A prospective natural-history study of coronary atherosclerosis. *N Engl J Med*. 2011;364:226–235.
23. Saia F, Komukai K, Capodanno D, Sirbu V, Musumeci G, Boccuzzi G, Tarantini G, Fineschi M, Tumminello G, Bernelli C, Niccoli G, Coccato M, Bordoni B, Bezerra H, Biondi-Zoccai G, Virmani R, Guagliumi G; OCTAVIA Investigators. Eroded versus ruptured plaques at the culprit site of STEMI: in vivo pathophysiological features and response to primary PCI. *JACC Cardiovasc Imaging*. 2015;8:566–575.
24. Dohi T, Mintz GS, McPherson JA, de Bruyne B, Farhat NZ, Lansky AJ, Mehran R, Weisz G, Xu K, Stone GW, Maehara A. Non-fibroatheroma lesion phenotype and long-term clinical outcomes: a substudy analysis from the prospect study. *JACC Cardiovasc Imaging*. 2013;6:908–916.

SUPPLEMENTAL MATERIAL

Data S1.

Supplemental Methods

OCT Image Acquisition and Analysis

Thrombectomy was performed with an aspiration catheter (Eliminate; Terumo, Tokyo, Japan or Export Advance; Medtronic, Minneapolis, MN, USA) to obtain TIMI 3 flow before optical coherence tomography (OCT) imaging. Either the time-domain (M2/M3 Cardiology Imaging System; LightLab Imaging, Inc., Westford, MA, USA) or the frequency-domain (C8-XRTM OCT Intravascular Imaging System; St. Jude Medical, St. Paul, MN, USA or LUNAWAVE™ OFDI System; Terumo, Tokyo, Japan) OCT system was used in the present study. The intracoronary OCT imaging technique is described elsewhere ¹⁻³. OCT images were analyzed by two independent investigators (M.H. and T.Y.) who were blinded to clinical information, and consensus reading was performed if there was disagreement in the interpretations. OCT analysis included either the presence or absence of intraluminal thrombus, plaque rupture (PR), thin cap fibroatheroma (TCFA), calcification, and macrophage infiltration according to consensus documents ^{1, 4, 5}. Massive thrombus was defined as a thrombus precluding visualization of underlying plaque morphology that was >90 degrees in circumference and >1 mm in length. Calcified nodule was characterized when fibrous cap disruption was detected over a calcified

plaque by protruding calcification, superficial calcium, and the presence of substantive calcium proximal and/or distal to the lesion ⁶.

Table S1. Characteristics of patients with and without MACE.

	MACE (n=85)	Without MACE (n=425)	P value
Age, y	64.0 (57.0-70.0)	67.0 (58.0-74.0)	0.129
Male	69 (81.2)	334 (78.6)	0.697
Hypertension	63 (74.1)	273 (64.2)	0.103
Dyslipidemia	39 (45.9)	214 (50.4)	0.526
Diabetes mellitus	31 (36.5)	137 (32.2)	0.527
Current smoker	42 (49.4)	177 (41.6)	0.230
Prior PCI	11 (12.9)	34 (8.0)	0.209
Prior MI	9 (10.6)	24 (5.6)	0.147
Ejection fraction, %	61.0 (55.0-64.0)	60.0 (52.0-65.0)	0.536
eGFR, mL/min/1.73m ²	69.4 (56.3-83.7)	73.1 (60.7-85.5)	0.239
Medication			
ACE/ARB	76 (89.4)	360 (84.9)	0.362
B blocker	53 (62.4)	286 (67.3)	0.450

Statin	68 (80.0)	376 (88.5)	0.052
Quantitative coronary angiography			
Reference vessel diameter	2.76 (2.55-3.10)	2.76 (2.32-3.21)	0.480
Minimum lumen diameter	0.61 (0.19-0.79)	0.56 (0.14-0.81)	0.877
Diameter stenosis	79.1 (69.4-93.0)	79.1 (69.9-92.6)	0.767
Lesion length	14.1 (10.5-17.2)	12.3 (9.7-15.6)	0.081
Procedural and angiographic			
2 nd generation DES	28 (32.9)	250 (58.8)	<0.001
Multi-vessel disease	38 (44.7)	141 (33.2)	0.047
AHA/ACC type B2/C	52 (61.2)	181 (42.6)	0.003
OCT finding			
LRP	83 (97.6)	364 (85.6)	<0.001
TCFA	57 (67.1)	197 (46.5)	<0.001
Thrombus volume	0.4 (0.0-2.7)	0.3 (0.0-1.5)	0.397
Culprit lesion morphology on OCT			
PR	65 (76.5)	263 (61.9)	0.002

IFC-LRP	18 (21.2)	104 (24.5)
IFC-non-LRP	2 (2.4)	58 (13.6)

Data are presented as n (%), mean SD, or median (interquartile range).

IFC indicates intact fibrous cap; PR, plaque rupture; LRP, lipid-rich plaque; ACE, angiotensin-converting enzyme inhibitors; ARB, angiotensin II Receptor Blocker; MACE, major advance cardiac events; DES indicates drug-eluting stent; PCI; percutaneous coronary intervention; MI, myocardial infarction; eGFR, estimated glomerular filtration rate; TCFA, thin-cap fibroatheroma; OCT, optical coherence tomography; MI; myocardial infarction; AHA, American Heart Association; ACC, American College of Cardiology.

Supplemental References:

1. Tearney GJ, Regar E, Akasaka T, Adriaenssens T, Barlis P, Bezerra HG, Bouma B, Bruining N, Cho JM, Chowdhary S, Costa MA, de Silva R, Dijkstra J, Di Mario C, Dudek D, Falk E, Feldman MD, Fitzgerald P, Garcia-Garcia HM, Gonzalo N, Granada JF, Guagliumi G, Holm NR, Honda Y, Ikeno F, Kawasaki M, Kochman J, Koltowski L, Kubo T, Kume T, Kyono H, Lam CC, Lamouche G, Lee DP, Leon MB, Maehara A, Manfrini O, Mintz GS, Mizuno K, Morel MA, Nadkarni S, Okura H, Otake H, Pietrasik A, Prati F, Raber L, Radu MD, Rieber J, Riga M, Rollins A, Rosenberg M, Sirbu V, Serruys PW, Shimada K, Shinke T, Shite J, Siegel E, Sonoda S, Suter M, Takarada S, Tanaka A, Terashima M, Thim T, Uemura S, Ughi GJ, van Beusekom HM, van der Steen AF, van Es GA, van Soest G, Virmani R, Waxman S, Weissman NJ, Weisz G, International Working Group for Intravascular Optical Coherence T. Consensus standards for acquisition, measurement, and reporting of intravascular optical coherence tomography studies: A report from the international working group for intravascular optical coherence tomography standardization and validation. *J Am Coll Cardiol.* 2012;59:1058-1072.
2. Prati F, Cera M, Ramazzotti V, Imola F, Giudice R, Giudice M, Propriis SD, Albertucci M. From bench to bedside: A novel technique of acquiring oct images. *Circulation journal : official journal of the Japanese Circulation Society.* 2008;72:839-843.

3. Prati F, Cera M, Ramazzotti V, Imola F, Giudice R, Albertucci M. Safety and feasibility of a new non-occlusive technique for facilitated intracoronary optical coherence tomography (oct) acquisition in various clinical and anatomical scenarios. *EuroIntervention*. 2007;3:365-370.
4. Prati F, Guagliumi G, Mintz GS, Costa M, Regar E, Akasaka T, Barlis P, Tearney GJ, Jang IK, Arbustini E, Bezerra HG, Ozaki Y, Bruining N, Dudek D, Radu M, Erglis A, Motreff P, Alfonso F, Toutouzas K, Gonzalo N, Tamburino C, Adriaenssens T, Pinto F, Serruys PW, Di Mario C, Expert's OCTRD. Expert review document part 2: Methodology, terminology and clinical applications of optical coherence tomography for the assessment of interventional procedures. *European heart journal*. 2012;33:2513-2520.
5. Prati F, Regar E, Mintz GS, Arbustini E, Di Mario C, Jang IK, Akasaka T, Costa M, Guagliumi G, Grube E, Ozaki Y, Pinto F, Serruys PW, Expert's OCTRD. Expert review document on methodology, terminology, and clinical applications of optical coherence tomography: Physical principles, methodology of image acquisition, and clinical application for assessment of coronary arteries and atherosclerosis. *Eur Heart J*. 2010;31:401-415.
6. Jia H, Abtahian F, Aguirre AD, Lee S, Chia S, Lowe H, Kato K, Yonetsu T, Vergallo R, Hu S, Tian J, Lee H, Park SJ, Jang YS, Raffel OC, Mizuno K, Uemura S, Itoh T, Kakuta

T, Choi SY, Dauerman HL, Prasad A, Toma C, McNulty I, Zhang S, Yu B, Fuster V, Narula J, Virmani R, Jang IK. In vivo diagnosis of plaque erosion and calcified nodule in patients with acute coronary syndrome by intravascular optical coherence tomography. *J Am Coll Cardiol.* 2013;62:1748-1758.